# Crack detection in concrete structures using standard deviation of discrete wavelet transform

Morteza Saadatmorad[1*], Samir Khatir[2], Bochra Khatir[3]

[1]Babol Noshirvani University of Technology, Babol, Iran
[2]Ho Chi Minh City Open University, Ho Chi Minh City, Vietnam
[3]University Center of Naama, Naama, Algeria
[*]Corresponding author: Eng.saadatmorad@gmail.com

**ARTICLE INFO**

**DOI:**10.46223/HCMCOUJS.acs.en.15.1.68.2025

Received: August 17th, 2024

Revised: October 10th, 2024

Accepted: October 17th, 2024

*Keywords*:

concrete structures; crack detection; optimal wavelet; standard deviation; wavelet transform

**ABSTRACT**

Crack detection in concrete structures is an important issue in the maintenance and repair operations of the structures. Detecting and distinguishing cracks in concrete can help determine the structure's health and prevent the possibility of structural failure. An efficient method for separating cracks in concrete is to use wavelet transform. This paper proposes a new crack detection technique based on a two-dimensional discrete wavelet transform and the standard deviation obtained from its detail signals to select an optimum wavelet function. According to our findings, there is a significant relation between the statistical index standard deviation and the desired detail signal obtained from the two-dimensional discrete wavelet transform for selecting the optimum wavelet function. Specifically, results show that as the standard deviation of the matrix of detail signal increases by a given wavelet function, crack detection resolution increases by that wavelet function.

## 1. Introduction

Structural crack detection based on image processing techniques is a suitable operation for structural health monitoring (Mohan & Poobal, 2018). Based on the desired crack detection, performing the desired maintenance and preserving operations is possible (Jo & Jadidi, 2020). Therefore, timely crack detection plays a determining role in presenting structural failure (Heshmati et al., 2022). Also, a proper crack separation algorithm can improve deep learning-based crack detection methods since it can highlight the main features of cracks.

So far, many studies have suggested using edge detection and machine learning algorithms to detect cracks in various structures. Saadatmorad, Rezaei-Sedehi, et al. (2024) proposed an improved edge detection method for detecting damage in historic structures. In this study, a Prewitt filter was improved. Fujita et al. (2006) proposed a noise cancellation technique for removing noises in concrete images. This method first eliminated noises such as blemishes, irregularly illuminated conditions, divots, and shading as a preprocessing operation; then, it applied the Hessian matrix to highlight the crack effects in images. Philip et al. (2023) conducted a comparative study for crack identification in concrete walls via a transfer learning approach. An automatic was proposed based on Convolutional Neural Networks (CNNs). The architectures VGG16, VGG19, Xception, ResNet50, and MobileNet were used in this study. According to their results, the architecture VGG16 demonstrated better accuracy and speed compared to the architecture VGG16. Then, the selected architecture VGG16 was compared to the architectures Xception, ResNet50, and MobileNet. Findings showed that the architecture Xception had the best performance for crack classification in concrete walls. Prasanna et al. (2014) proposed an automatic crack identification procedure for concrete bridges. A robot collected input images of machine learning classifiers such as random forest and Support Vector Machine (SVM). They named their technique as Spatially Tuned Robust Multifeature (STRUM). Their proposed method showed 95% accuracy in classifying cracks on concrete bridges. Crack detection by human naked eyes has a series of difficulties and errors such as crack misidentification, data evaluation inefficiency, slow detection, and subjectivity. Thus, Yu et al. (2007) suggested a crack inspection method using image processing to overcome common human errors for crack detection. They tested their methodology on a subway tunnel, a road tunnel, and an indoor structure to measure cracks in concrete structures based on a mobile robot system equipped with a Charged Couple Device (CCD) camera for acquiring image data. Cho et al. (2018) proposed an edge-based crack detection technique containing five steps for transforming, filling, and removing pixels for robust crack detection. They named their method the Crack Width Transform (CWT).

Wavelet transform is a signal processing tool that can be used for crack detection. Surace and Ruotolo (1994) studied crack detection in beam structures using the One-Dimensional Continuous Wavelet Transform (1D-CWT). The cracked beam's data was obtained from the finite element model. This research demonstrated the efficiency of wavelet transforms for detecting abrupt changes in signals. Saadatmorad et al. (2022) studied crack detection in steel beam structures using One-Dimensional Discrete Wavelet Transform (1D-DWT) and Pearson correlation. They processed the vibrational mode shape signal of steel cracked beams through the Pearson correlation filter to feed them in the 1D-DWT. Findings showed the proposed method acted better than just using the 1D-DWT. Kobylin and Lyashenko (2014) compared classical image edge detection methods such as Prewitt, Robert, Canny, and Sobel with Two-Dimensional Continuous Wavelet Transform (2D-CWT). Findings showed that although the classical methods were better in terms of computational effort, the 2D-CWT presented a better quality of edge detection. Thus, a combined approach can be more helpful. Divakar et al. (2022) studied image pattern recognition via edge detection based on the two-dimensional wavelet transform. They implied the edges as high-frequency parts of images representing where abrupt change takes place in the intensity of luminescence. Edge detection was addressed as an essential step for feature extraction or pattern recognition in images. The ability of the two-dimensional wavelet transform to separate high-frequency and low-frequency parts of images was addressed in this study.

In this paper, statistical evaluations are performed on the matrix of detail signals obtained from the two-dimensional wavelet transform to determine the statistical index sensitive to the crack resolution separated by the discrete two-dimensional wavelet transform. We use different wavelet functions and then compare the statistical indices of the detail signal obtained from them to discover which statistical index of the detail signal is sensitive to crack detection accuracy. Finally, we introduce this index as a criterion for choosing the optimal wavelet function. The benefit of the proposed method are:

- Discovering the best wavelet function for crack detection.
- Proposing an optimal crack detection methodology of concrete structures.

## 2. One-dimensional wavelet transform

By definition, a wavelet $\psi(t)$ is an oscillatory function that satisfies the following conditions:

$$\int_{-\infty}^{+\infty} \psi(t)dt = 0 \tag{1}$$

$$\int_{-\infty}^{+\infty} |\psi(t)|^2 \, dt < \infty \tag{2}$$

where the relations (1) and (2) are the zero mean and finite energy conditions, respectively. One-dimensional continuous wavelet transform is expressed as follows:

$$CWT_{a,b} = \frac{1}{\sqrt{a}} \int_{-\infty}^{+\infty} f(t) \psi(\frac{t-b}{a}) dt \tag{3}$$

where $CWT_{a,b}$ denote the wavelet coefficients obtained from the One-dimensional continuous wavelet transform. $f(t)$ is a function with a continuous time or space variable $t$. Also, $a$ is the scaling parameter and $b$ is the shifting parameter. $\psi_{a,b}(t) = \psi\left(\frac{t-b}{a}\right)$ shows the scaled and shifted family of the wavelet function $\psi(t)$. Note that $\frac{1}{\sqrt{a}}$ is the normalization factor of the wavelet transform. It influences the generated wavelet coefficient at each given scale. Thus, as $a$ increases, the wavelet function $\psi(t)$ becomes wider and the wavelet coefficients are multiplied by a smaller number. Numerical experiences have proven that the higher scales are unsuitable for detecting abrupt local changes in signals. Thus, a selection method for the desired scale is required. For fixing this problem, by setting $a = 2^j$ and $b = ak$, discrete family of wavelets are rewritten as follows:

$$\psi_{j,k}(t) = \psi\left(2^{-j}t - k\right) \tag{4}$$

Thus, one-dimensional discrete wavelet transform is expressed as follows:

$$DWT_{j,k} = \frac{1}{\sqrt{2^j}} \int_{-\infty}^{+\infty} f(t) \psi\left(2^j t - k\right) dt \tag{5}$$

where $DWT_{j,k}$ denote the wavelet coefficients obtained from the One-dimensional discrete wavelet transform.

The multiresolution analysis is used to decompose the original signal $f(t)$ into sub-signals to implement the discrete wavelet transform. Therefore, a theory about relations between the space of square-integrable functions $L^2(\mathbb{R})$ and its closed subspaces $S_j$ is addressed (Divakar et al., 2022):

$$\cup S_j \ = L^2(\mathbb{R}), \qquad \forall \ j\epsilon\mathbb{Z} \tag{6}$$

$$\cap S_j \ = \{0\}, \qquad \forall \ j\epsilon\mathbb{Z} \tag{7}$$

$$S_{j+1} \subset S_j \quad , \qquad \forall \ j\epsilon\mathbb{Z} \tag{8}$$

$$f(t) \in S_j \rightarrow f(2t) \in S_{j+1} \quad , \qquad \forall \ j\epsilon\mathbb{Z} \tag{9}$$

$$\varphi(t)\epsilon S_0 \rightarrow \{\varphi(t-k)\} \perp S_0 \tag{10}$$

where $\varphi(t)$ is the scaling function. Inspiring the above relations, the pyramidal decomposition can be performed as follows (Saadatmorad, Shahavi, et al., 2024):

$$f(t) = A_j(t) + \sum_{m=1}^{j} d_m(t) \tag{11}$$

where $A_j(t)$ is an approximation function of the original function $f(t)$. Also, $d_m(t)$ are the detail signal(s) of the original function $f(t)$.

We obtain these signals using the following relations:

$$d_m(t) = \sum_{n=-\infty}^{\infty} C_{detail}(m,n)\psi(t)_{m,n} \tag{12}$$

$$A_j(t) = \sum_{n=-\infty}^{+\infty} C_{approximation}(j,n)\varphi_{j,n}(t) \tag{13}$$

where $C_{detail}$ and $C_{approximation}$ are the detail and approximation coefficients.

**3. Formulation**

This section deals with our methodology. First, we expand the 1D-DWT to 1D-DWT by the following tensor products:

$$\phi(t_1,t_2) = \phi(t_1)\phi(t_2) \tag{14}$$

$$\psi^D(t_1,t_2) = \psi(t_1)\,\psi(t_2) \tag{15}$$

where $\phi(t_1,t_2)$ is two-dimensional scaling function and $\psi^D(t_1,t_2)$ is two-dimensional diagonal wavelet function. These functions can act as the filter to process the two-dimensional signals or images. Thus, the two-dimensional signal $f(t_1,t_2)$ is divided into four sub-images. These four images are respectively $\mathrm{A}^{\Phi}{}_{\mathrm{j,m,n}}(t_1,t_2)$as approximate image,$\mathrm{D}^{\mathrm{H}}{}_{\mathrm{j,m,n}}(t_1,t_2)$ as horizontal detail image, $\mathrm{D}^{\mathrm{V}}{}_{\mathrm{j,m,n}}(t_1,t_2)$ as vertical detail image, and $\mathrm{D}^{\mathrm{D}}{}_{\mathrm{j,m,n}}(t_1,t_2)$ as diagonal detail image. Assuming the size of $f(t_1,t_2)$ is $\mathrm{n} \times \mathrm{m}$, the following relations are related to the two-dimensional discrete wavelet transform:

$$A^{\phi}{}_{j,m,n}(t_1,t_2) = \frac{1}{\sqrt{mn}} \sum_{i=0}^{m-1} \sum_{q=0}^{n-1} f(t_1,t_2) 2^{\frac{-j}{2}} \phi(2^{-j}t_1 - m, 2^{-j}t_2 - n) \tag{16}$$

$$D_{H\,j,m,n}(t_1,t_2) = \frac{1}{\sqrt{mn}} \sum_{i=0}^{m-1} \sum_{q=0}^{n-1} f(t_1,t_2) 2^{\frac{-j}{2}} \psi(2^{-j}t_1 - m, 2^{-j}t_2 - n) \tag{17}$$

$$D_{V\,j,m,n}(t_1,t_2) = \frac{1}{\sqrt{mn}} \sum_{i=0}^{m-1} \sum_{q=0}^{n-1} f(t_1,t_2) 2^{\frac{-j}{2}} \psi(2^{-j}t_1 - m, 2^{-j}t_2 - n) \tag{18}$$

$$D_{D\,j,m,n}(t_1,t_2) = \frac{1}{\sqrt{mn}} \sum_{i=0}^{m-1} \sum_{q=0}^{n-1} f(t_1,t_2) 2^{\frac{-j}{2}} \psi(2^{-j}t_1 - m, 2^{-j}t_2 - n) \tag{19}$$

Consider a detail matrix $\mathrm{D}_{\mathrm{m}\times\mathrm{n}}$ as follows:

$$D_{m\times n}=\begin{bmatrix} d_{1\,1} & d_{1\,2} & d_{1\,3} & & d_{1n-2} & d_{1\,n-1} & d_{1\,n} \\ d_{2\,1} & d_{2\,2} & d_{2\,3} & \cdots & d_{2\,n-2} & d_{2\,n-1} & d_{2\,n} \\ d_{3\,1} & d_{3\,2} & d_{3\,3} & & d_{3\,n-2} & d_{3\,n-1} & d_{3\,n} \\ & \vdots & & \ddots & & \vdots & \\ d_{m-2\,1} & d_{m-2\,2} & d_{m-2\,3} & & d_{m-2\,n-2} & d_{m-2\,n-1} & d_{m-2\,n} \\ d_{m-1\,1} & d_{m-1\,2} & d_{m-1\,3} & \cdots & d_{m-1\,n-2} & d_{m-1\,n-1} & d_{m-1\,n} \\ d_{m\,1} & d_{m\,2} & d_{m\,3} & & d_{m\,n-2} & d_{m\,n-1} & d_{mn} \end{bmatrix} \tag{20}$$

We compute the standard deviation of the detail signal. Because the detail signals are two-dimensional, we have to compute the standard deviation of the matrix. For this, we compute the standard deviation of each column of detail signal at first as follows:

$$C=\begin{Bmatrix} C_1 \\ C_2 \\ C_3 \\ \vdots \\ . \\ C_{n-2} \\ C_{n-1} \\ C_n \end{Bmatrix}=\begin{Bmatrix} \sqrt{\frac{1}{m-1}\sum_{i=1}^{m}\left| d_{i\,1} - \frac{1}{m-1}\sum_{i=1}^{m} d_{i\,1}\right|^2} \\ \sqrt{\frac{1}{m-1}\sum_{i=1}^{m}\left| d_{i\,2} - \frac{1}{m-1}\sum_{i=1}^{m} d_{i\,2}\right|^2} \\ \sqrt{\frac{1}{m-1}\sum_{i=1}^{m}\left| d_{i\,3} - \frac{1}{m-1}\sum_{i=1}^{m} d_{i\,3}\right|^2} \\ \vdots \\ \sqrt{\frac{1}{m-1}\sum_{i=1}^{m}\left| d_{i\,n-2} - \frac{1}{m-1}\sum_{i=1}^{m} d_{i\,n-2}\right|^2} \\ \sqrt{\frac{1}{m-1}\sum_{i=1}^{m}\left| d_{i\,n-1} - \frac{1}{m-1}\sum_{i=1}^{m} d_{i\,n-1}\right|^2} \\ \sqrt{\frac{1}{m-1}\sum_{i=1}^{m}\left| d_{i\,n} - \frac{1}{m-1}\sum_{i=1}^{m} d_{i\,n}\right|^2} \end{Bmatrix} \tag{21}$$

Finally, the standard deviation of the detail matrix is computed as follows:

$$STD_D=\sqrt{\frac{1}{n-1}\sum_{i=1}^{n}\left| C_i - \frac{1}{n-1}\sum_{i=1}^{n} C_i\right|^2} \tag{22}$$

We select the detail signal with a wavelet function that provides the maximum standard deviation for crack detection objectives.

## 4. Results

As mentioned, the proposed methodology decomposes the image of the concrete structure into an approximation image and three detail images in the vertical, horizontal, and diagonal directions. With this method, it is possible to track cracks in the concrete structure in different directions. To check the performance of the proposed methodology, four damage scenarios corresponding to four structure samples containing cracks with different patterns are examined.

**Figure 1**

*The Original Image and Its Corresponding Detail Signals for the Scenario 1*

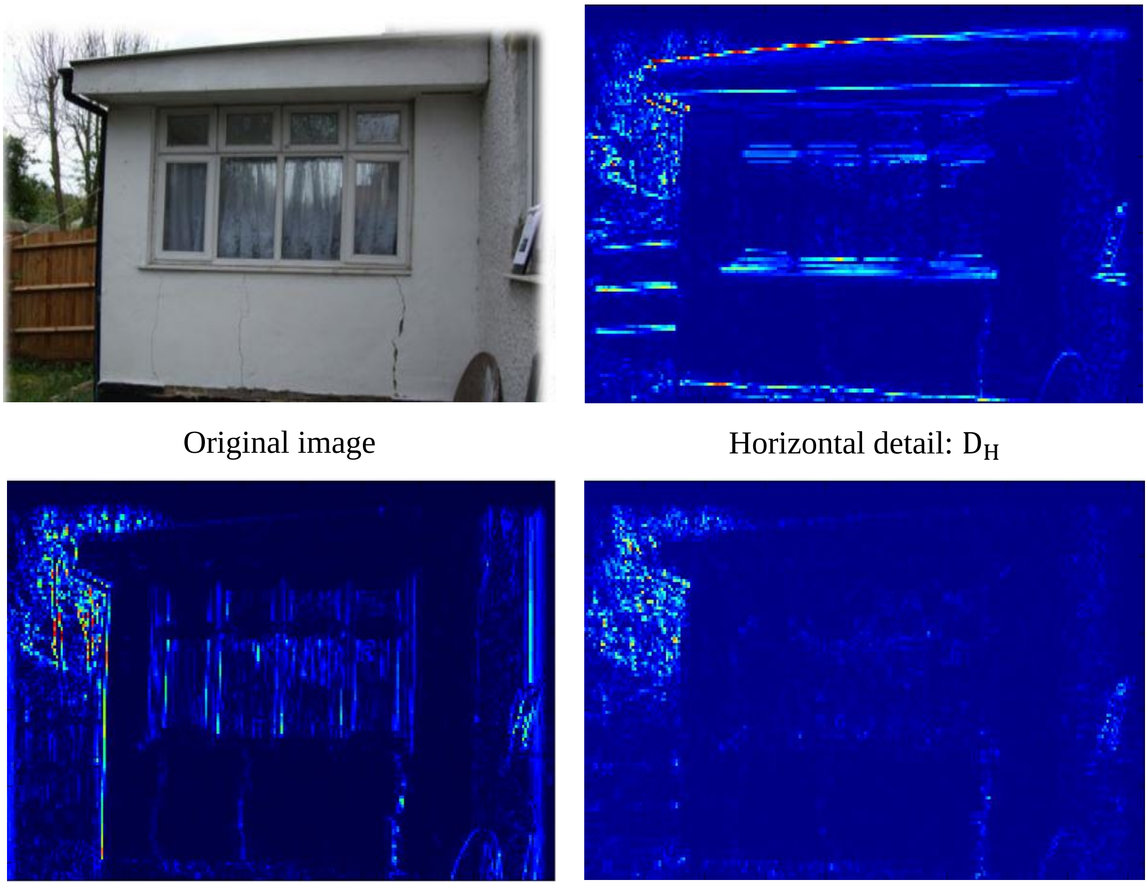

Original image

Horizontal detail: $D_H$

Vertical detail: $D_V$

Diagonal detail: $D_D$

*Source.* Original image from https://daviespropertysolutions.com

Figure 1 shows the first structure under investigation as the first damage scenario with the three details signals. As seen, the horizontal edges in the structure are well separated and identified. The vertical cracks in the structure are visible. According to Figure 1, the detail signals give a better view for separating cracks in different directions than the original image. There are three vertical cracks in the original images that are detected with high accuracy in Figure 1. In this scenario, the Haar wavelet function was used to process the original image. According to the results, crack separation by observing the details of the discrete wavelet transform is much easier than observing the original image. Thus, the best detail signal for scenario 1 is the vertical signal, and we can investigate the optimal wavelet selection process on this detail signal. To evaluate the second scenario, Figure 2 shows the vertical, horizontal, and diagonal details corresponding to a concrete bridge structure. The vertical detail identifies the vertical crack in the concrete bridge structure. According to the other detail signals, there are no horizontal and diagonal cracks. Therefore, the vertical detail of the two-dimensional discrete wavelet transform is used for crack identification, and the horizontal and diagonal directions guarantee the absence of horizontal and diagonal cracks in the concrete structure, respectively. Thus, the best detail signal for scenario 2 is the vertical signal, and we can investigate the optimal wavelet selection process on this detail signal.

**Figure 2**

*The Original Image and Its Corresponding Detail Signals for the Scenario 2*

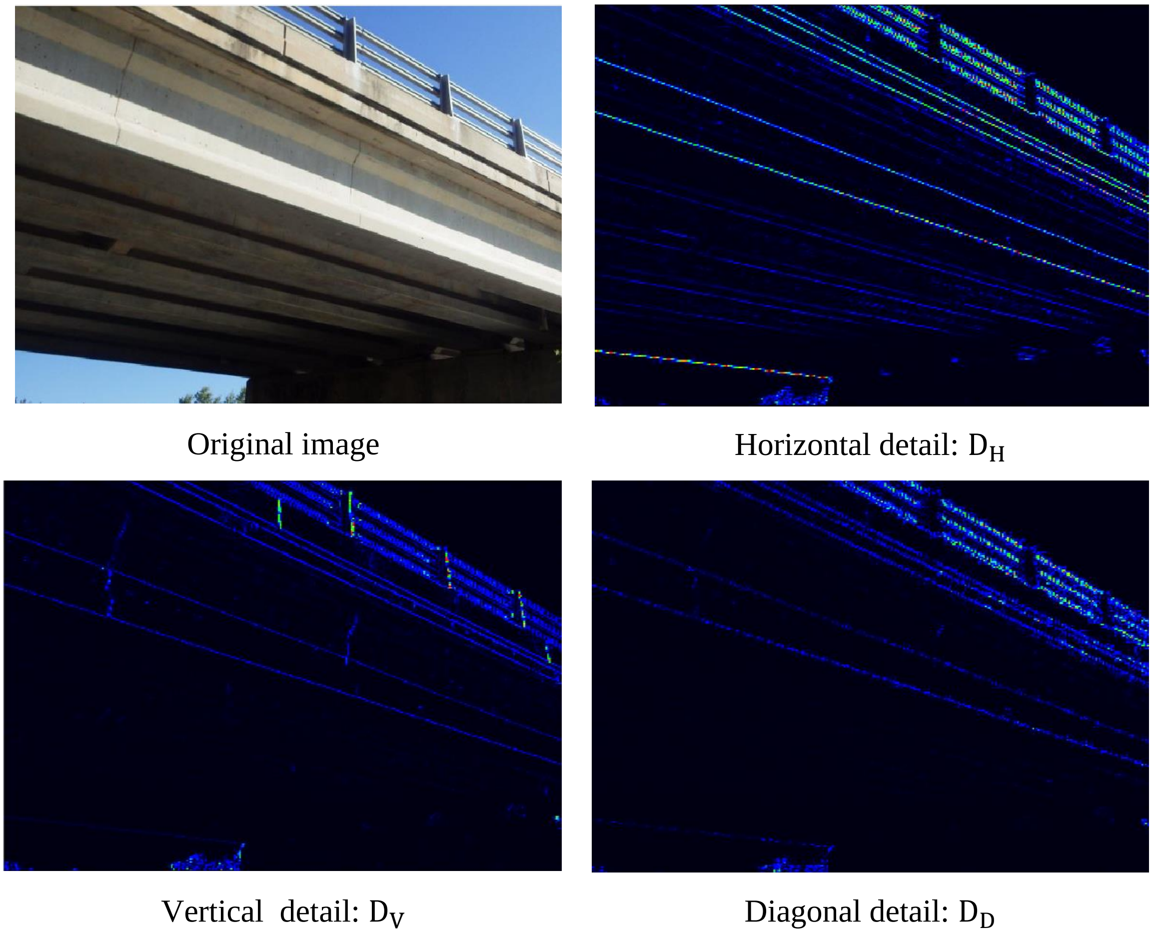


*Source.* Original image from https://www.picketplacebridge.com

To evaluate the effectiveness of the proposed method, in this section, statistical research is presented to select the best wavelet function and the effect of choosing the optimal wavelet function on the accuracy of crack detection results. The desired index for the optimality of the wavelet function is the standard deviation of the images of the detail signals. It is important to note that increasing the standard deviation of an image matrix means that the values within the matrix become wider or more variable. In other words, as the standard deviation increases, the data points in the image matrix deviate more from the mean. For example, if the image matrix has a lower standard deviation, the values are clustered closer to the mean. On the other hand, a matrix with a higher standard deviation indicates that the values are wider and farther from the mean. In practical terms, an increase in the standard deviation of a matrix can indicate greater variability or dispersion in the data, which may have implications for statistical analysis, quality control, or other applications where understanding data variability is important. Figure 3 indicates the results of the two-dimensional wavelet transform corresponding to six different wavelet functions (i.e., Haar, Db3, Sym4, Coif3, Bior 3.9, and Dmey) for the first damage scenario. We use different wavelet families with different vanishing moments to capture both the effect of the wavelet family and the vanishing moments of the wavelet functions.

**Figure 3**

*The Results of the Two-Dimensional Wavelet Transform for the First Scenario*

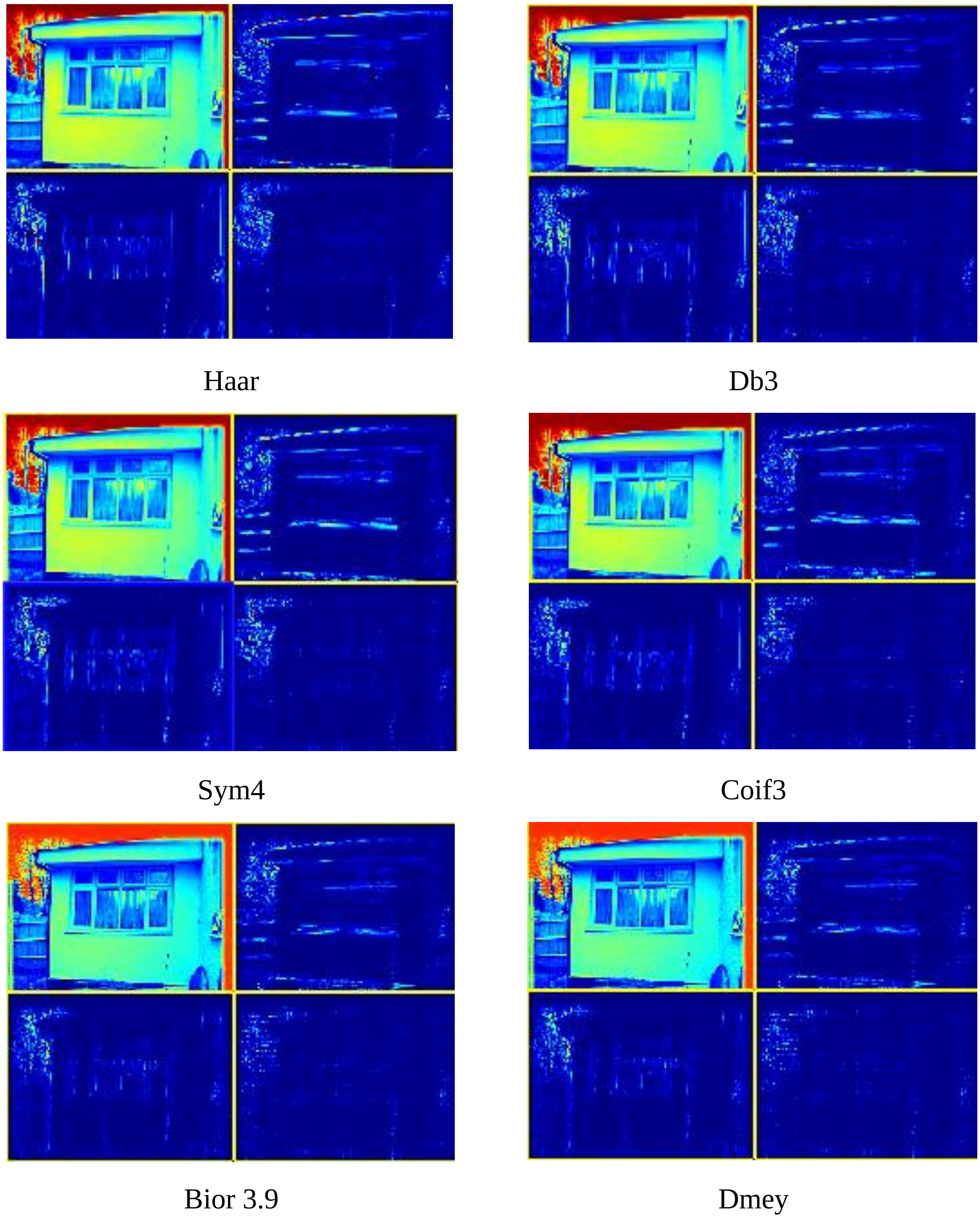


*Source.* Original image from https://daviespropertysolutions.com

Figure 4 shows the statistical results corresponding to the visual results presented in Figure 3. By observing the resolution of the crack areas in the images provided by the wavelet transform, comparing the results presented in Figures 3 and 4 shows that as the standard deviation of detail signals increases, the ability of edge detection and crack detection increases. The best crack detection in Figure 3 is related to the wavelet function Haar. At the same time, the highest value of the standard deviation in Figure 4 is related to the wavelet function Haar, as well.

**Figure 4**

*Statistical Results Corresponding to the Results Presented in Figure 3*

Haar

| | | | | | | | |
|---|---|---|---|---|---|---|---|
| Mean | 0 | Maximum | 61.5 | Standard dev. | 5.311 | L1 norm | 2.75e+05 |
| Median | 0 | Minimum | -61.5 | Median Abs. Dev. | 0.5 | L2 norm | 1846 |
| Mean | 1.23 | Range | 123 | Mean Abs. Dev. | 2.276 | Max norm | 61.5 |

Db3

| | | | | | | | |
|---|---|---|---|---|---|---|---|
| Mean | 0.003501 | Maximum | 75.37 | Standard dev. | 3.664 | L1 norm | 1.848e+05 |
| Median | 5.405e-10 | Minimum | -65.54 | Median Abs. Dev. | 0.4076 | L2 norm | 1274 |
| Mean | 0.6882 | Range | 140.9 | Mean Abs. Dev. | 1.529 | Max norm | 75.37 |

Sym4

| | | | | | | | |
|---|---|---|---|---|---|---|---|
| Mean | -0.003193 | Maximum | 55.82 | Standard dev. | 3.47 | L1 norm | 1.778e+05 |
| Median | 2.04e-10 | Minimum | -58.75 | Median Abs. Dev. | 0.3826 | L2 norm | 1206 |
| Mean | -0.3213 | Range | 114.6 | Mean Abs. Dev. | 1.472 | Max norm | 58.75 |

Coif 3

| | | | | | | | |
|---|---|---|---|---|---|---|---|
| Mean | -0.002485 | Maximum | 52.79 | Standard dev. | 3.339 | L1 norm | 1.719e+05 |
| Median | 8.749e-07 | Minimum | -61.19 | Median Abs. Dev. | 0.3857 | L2 norm | 1161 |
| Mean | -0.7788 | Range | 114 | Mean Abs. Dev. | 1.423 | Max norm | 61.19 |

Bior 3.9

| | | | | | | | |
|---|---|---|---|---|---|---|---|
| Mean | 0 | Maximum | 56.79 | Standard dev. | 3.376 | L1 norm | 1.755e+05 |
| Median | 0 | Minimum | -57 | Median Abs. Dev. | 0.4114 | L2 norm | 1174 |
| Mean | 1.036 | Range | 113.8 | Mean Abs. Dev. | 1.452 | Max norm | 57 |

Dmey

| | | | | | | | |
|---|---|---|---|---|---|---|---|
| Mean | -0.0008326 | Maximum | 54.79 | Standard dev. | 3.225 | L1 norm | 1.771e+05 |
| Median | 0.0002731 | Minimum | -52.63 | Median Abs. Dev. | 0.4484 | L2 norm | 1121 |
| Mean | 0.004721 | Range | 107.4 | Mean Abs. Dev. | 1.465 | Max norm | 54.79 |

*Source.* Data analysis result of the research

Likewise, the wavelet functions that produce the detail signals with higher standard deviations detect cracks with higher accuracy.

Figure 5 denotes indicates the results of the two-dimensional wavelet transform corresponding to six different wavelet functions (i.e., Haar, Db3, Sym4, Coif3, Bior 3.9, and Dmey) for the first damage scenario. Again, we use different wavelet families with different vanishing moments to have the effects of the wavelet family and the vanishing moments of the wavelet functions.

**Figure 5**

*The Results of the Two-Dimensional Wavelet Transform for the Second Scenario*

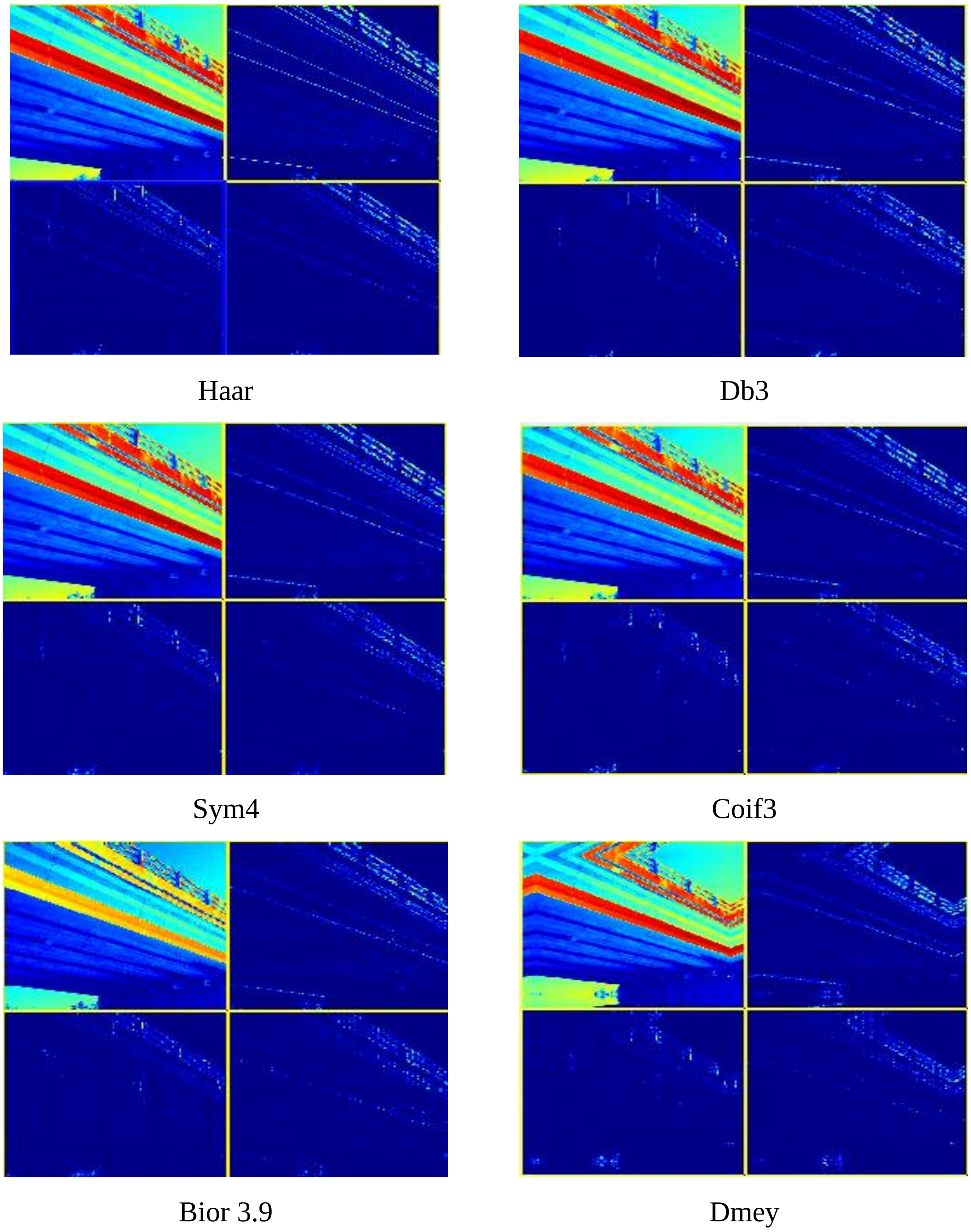


*Source.* Original image from https://www.picketplacebridge.com

Figure 6 present the statistical results of the visual results presented in Figure 5. Comparing the results presented in Figures 5 and 6 shows that as the standard deviation of detail signals increases, the ability of edge detection and crack detection increases. The best crack detection in Figure 5 is related to the wavelet function Haar. At the same time, the highest value of the standard deviation in Figure 6 is related to the wavelet function Haar, as well. Again, it is obvious that the wavelet functions that generate the detail signals with higher standard deviations can detect cracks with higher accuracy.

**Figure 6**

*Statistical Results Corresponding to the Results Presented in Figure 5*

Haar

| | | | | | | | |
|---|---|---|---|---|---|---|---|
| Mean | 0 | Maximum | 79.5 | Standard dev. | 3.402 | L1 norm | 3.804e+05 |
| Median | 0 | Minimum | -79.5 | Median Abs. Dev. | 0.25 | L2 norm | 1921 |
| Mean | 1.59 | Range | 159 | Mean Abs. Dev. | 1.193 | Max norm | 79.5 |

Db3

| | | | | | | | |
|---|---|---|---|---|---|---|---|
| Mean | 4.488e-05 | Maximum | 83.17 | Standard dev. | 2.13 | L1 norm | 2.367e+05 |
| Median | -0.002083 | Minimum | -68.04 | Median Abs. Dev. | 0.2675 | L2 norm | 1202 |
| Mean | 0.004102 | Range | 151.2 | Mean Abs. Dev. | 0.7425 | Max norm | 83.17 |

Sym4

| | | | | | | | |
|---|---|---|---|---|---|---|---|
| Mean | -4.357e-05 | Maximum | 71.18 | Standard dev. | 1.991 | L1 norm | 2.088e+05 |
| Median | 0.0008345 | Minimum | -66.35 | Median Abs. Dev. | 0.2361 | L2 norm | 1124 |
| Mean | 1.041 | Range | 137.5 | Mean Abs. Dev. | 0.6543 | Max norm | 71.18 |

Coif 3

| | | | | | | | |
|---|---|---|---|---|---|---|---|
| Mean | -4.748e-05 | Maximum | 63.79 | Standard dev. | 1.864 | L1 norm | 2.001e+05 |
| Median | 0.002124 | Minimum | -65.01 | Median Abs. Dev. | 0.2407 | L2 norm | 1052 |
| Mean | 0.6788 | Range | 128.8 | Mean Abs. Dev. | 0.6278 | Max norm | 65.01 |

Bior 3.9

| | | | | | | | |
|---|---|---|---|---|---|---|---|
| Mean | 0 | Maximum | 62.38 | Standard dev. | 1.892 | L1 norm | 2.186e+05 |
| Median | -0.0005073 | Minimum | -66.73 | Median Abs. Dev. | 0.2714 | L2 norm | 1068 |
| Mean | -0.888 | Range | 129.1 | Mean Abs. Dev. | 0.6857 | Max norm | 66.73 |

Dmey

| | | | | | | | |
|---|---|---|---|---|---|---|---|
| Mean | -4.852e-05 | Maximum | 50.6 | Standard dev. | 1.736 | L1 norm | 2.02e+05 |
| Median | 0.001008 | Minimum | -55.7 | Median Abs. Dev. | 0.2557 | L2 norm | 980.3 |
| Mean | 0.6411 | Range | 106.3 | Mean Abs. Dev. | 0.6335 | Max norm | 55.7 |

*Source.* Data analysis result of the research

**Figure 7**

*The Results of the Two-Dimensional Wavelet Transform for the Third Scenario*

Original image

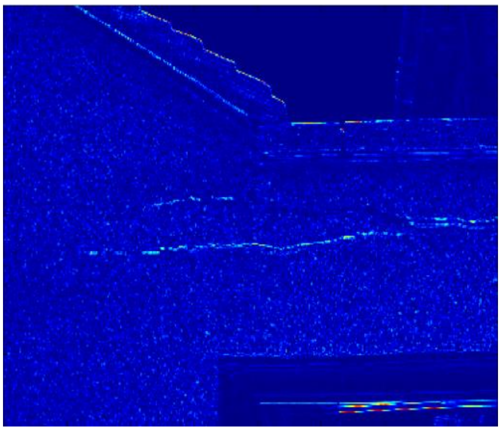

Haar

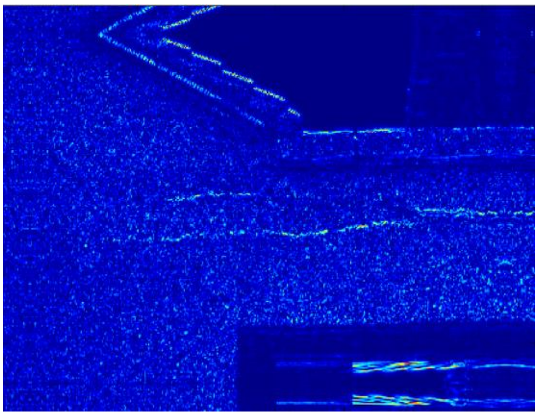

Dmey

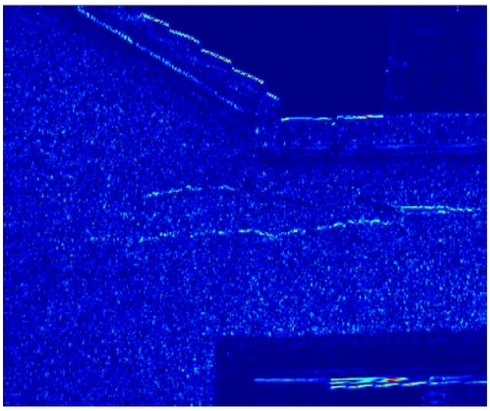

Sym7

*Source.* Original image from https://www.designingbuildings.co.uk

**Figure 8**

*Statistical Results Corresponding to the Results Presented in Figure 7*

Haar

| | | | | | | | |
|---|---|---|---|---|---|---|---|
| Mean | 0 | Maximum | 99.82 | Standard dev. | 7.384 | L1 norm | 2.198e+06 |
| Median | 0 | Minimum | -99.82 | Median Abs. Dev. | 3.07 | L2 norm | 5054 |
| Mean | 1.996 | Range | 199.6 | Mean Abs. Dev. | 4.691 | Max norm | 99.82 |

Dmey

| | | | | | | | |
|---|---|---|---|---|---|---|---|
| Mean | 6.725e-06 | Maximum | 57.13 | Standard dev. | 6.481 | L1 norm | 2.04e+06 |
| Median | 9.05e-05 | Minimum | -68.38 | Median Abs. Dev. | 2.908 | L2 norm | 4437 |
| Mean | 0.6516 | Range | 125.5 | Mean Abs. Dev. | 4.353 | Max norm | 68.38 |

Sym7

| | | | | | | | |
|---|---|---|---|---|---|---|---|
| Mean | -4.438e-06 | Maximum | 65.81 | Standard dev. | 6.576 | L1 norm | 1.987e+06 |
| Median | 5.598e-10 | Minimum | -84.3 | Median Abs. Dev. | 2.657 | L2 norm | 4501 |
| Mean | 1.265 | Range | 150.1 | Mean Abs. Dev. | 4.241 | Max norm | 84.3 |

*Source.* Data analysis result of the research

**Figure 9**

*The Results of the Two-Dimensional Wavelet Transform for the Fourth Scenario*

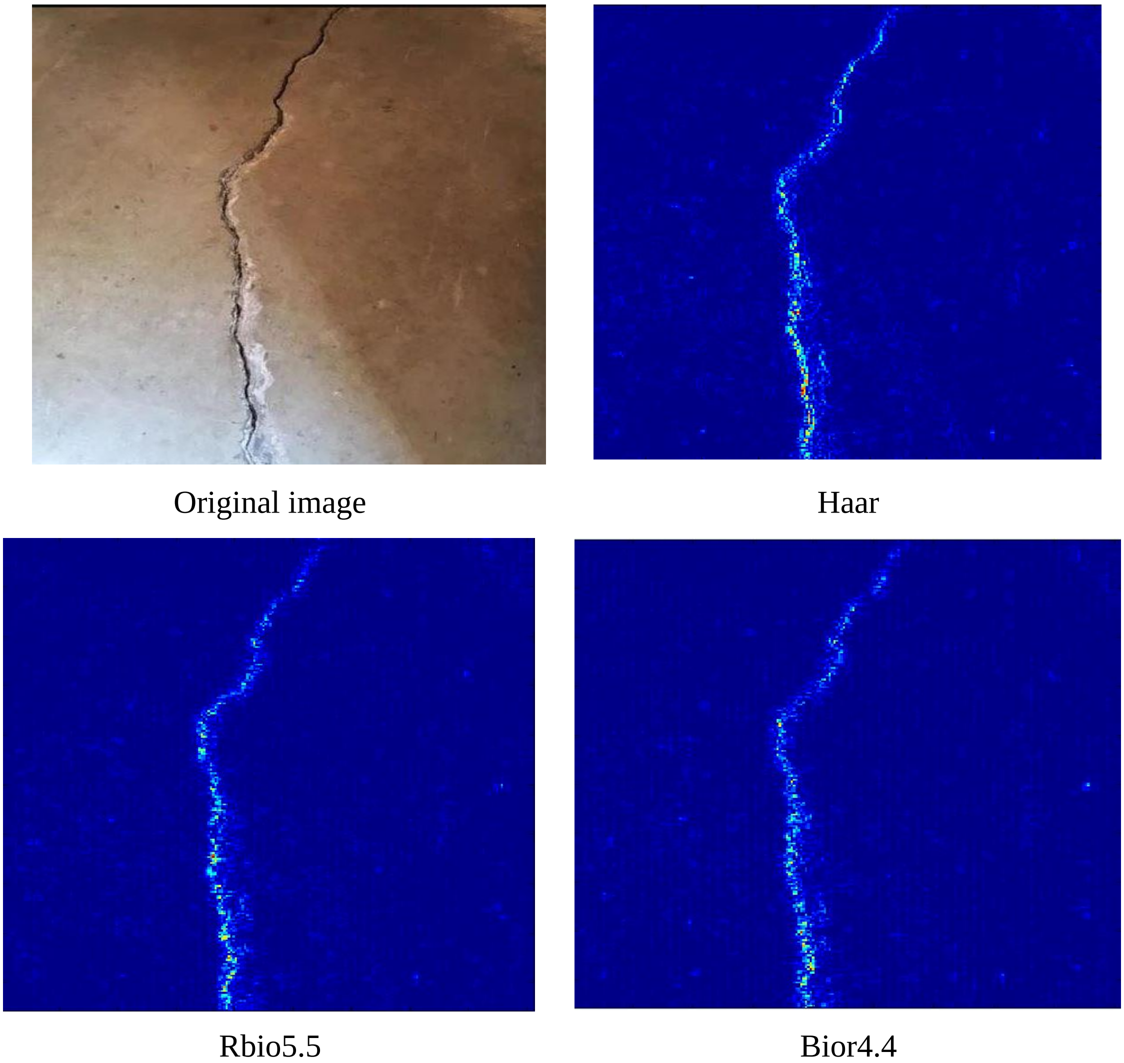


*Source.* Original image from https://www.pinterest.com

**Figure 10**

*Statistical Results Corresponding to the Results Presented in Figure 9*

Haar

| | | | | | | | |
|---|---|---|---|---|---|---|---|
| Mean | 0.001492 | Maximum | 39 | Standard dev. | 1.672 | L1 norm | 3.096e+04 |
| Median | 0 | Minimum | -34 | Median Abs. Dev. | 0.299 | L2 norm | 390.2 |
| Mean | 0.31 | Range | 73 | Mean Abs. Dev. | 0.5688 | Max norm | 39 |

Rbio5.5

| | | | | | | | |
|---|---|---|---|---|---|---|---|
| Mean | 0.001775 | Maximum | 23.57 | Standard dev. | 0.968 | L1 norm | 2.198e+04 |
| Median | 0.00117 | Minimum | -18.92 | Median Abs. Dev. | 0.2051 | L2 norm | 226 |
| Mean | 0.1974 | Range | 42.49 | Mean Abs. Dev. | 0.4033 | Max norm | 23.57 |

Bior4.4

| | | | | | | | |
|---|---|---|---|---|---|---|---|
| Mean | 0.001752 | Maximum | 29.54 | Standard dev. | 1.022 | L1 norm | 2.314e+04 |
| Median | 4.739e-11 | Minimum | -27.45 | Median Abs. Dev. | 0.2298 | L2 norm | 238.5 |
| Mean | 0.4755 | Range | 56.99 | Mean Abs. Dev. | 0.4247 | Max norm | 29.54 |

*Source.* Data analysis result of the research

## 5. Discussion

Two-dimensional discrete wavelet transform is a qualitative method for feature extraction. It only reacts to the magnitude of local contrasts to detect local jumps. Therefore, it is not dependent on the dimensions of the structural samples. Also, in the analysis of crack images, it is sensitive to local resolution changes and it is obvious that if the lighting conditions are such that this contrast is affected. In light conditions such as shadow, these local signal changes are not noticeable, and as a result, the edge detection performance by wavelet transform changes. In this paper, all important wavelet functions in Matlab software were tested to discover the relation between the increase in standard deviation of wavelet coefficients and the increase in accuracy (or resolution) of crack detection in concrete structures. A major limitation or drawback of the proposed method is to provide an original image without shadow and noise on the cracks and close enough to the crack. In this paper, both hairline cracks and structural cracks were investigated in horizontal, vertical, and diagonal directions in this research.

## 6. Conclusions

Accurate crack detection of concrete structures can be helpful for repairing and maintaining them. In this regard, a new wavelet selection criterion is proposed. The proposed criterion is based on the standard deviation of detail signals obtained from the two-dimensional discrete wavelet transform. It is found that as the standard deviation of the two-dimensional detail signals obtained from a given wavelet function increases, the ability of that wavelet function for accurate crack detection increases. According to the results, the Haar wavelet function is the best wavelet function for crack detection, especially for vertical cracks considered in this paper. This optimal wavelet selection criterion can be useful for improving computer vision-based machine learning algorithms for edge detection and crack detection tasks.

## References

Cho, H., Yoon, H. J., & Jung, J. Y. (2018). Image-based crack detection using Crack Width Transform (CWT) algorithm. *Institute of Electrical and Electronics Engineers Access*, *6*(1), 60100-60114.

Divakar, R., Singh, B., Bajpai, A., & Kumar, A. (2022). Image pattern recognition by edge detection using discrete wavelet transforms. *Journal of Decision Analytics and Intelligent Computing, 2*(1), 26-35.

Fujita, Y., Mitani, Y., & Hamamoto, Y. (2006). A method for crack detection on a concrete structure. *18th International Conference on Pattern Recognition (ICPR'06), 3*, 901-904.

Heshmati, A., Saadatmorad, M., Talookolaei, R. A. J., Valvo, P. S., & Khatir, S. (2022). Damage identification in thin steel beams containing a horizontal crack using the artificial neural networks. In *International conference of steel and composite for engineering structures* (pp. 114-126). Springer International Publishing.

Jo, J., & Jadidi, Z. (2020). A high precision crack classification system using multi-layered image processing and deep belief learning. *Structure and Infrastructure Engineering, 16*(2), 297-305.

Kobylin, O., & Lyashenko, V. (2014). Comparison of standard image edge detection techniques and of method based on wavelet transform. *International Journal of Advanced Research, 2*(8), 572-580.

Mohan, A., & Poobal, S. (2018). Crack detection using image processing: A critical review and analysis. *Alexandria Engineering Journal, 57*(2), 787-798.

Philip, R. E., Andrushia, A. D., Nammalvar, A., Gurupatham, B. G. A., & Roy, K. (2023). A comparative study on crack detection in concrete walls using transfer learning techniques. *Journal of Composites Science, 7*(4), Article 169.

Prasanna, P., Dana, K. J., Gucunski, N., Basily, B. B., La, H. M., Lim, R. S., & Parvardeh, H. (2014). Automated crack detection on concrete bridges. *IEEE Transactions on Automation Science and Engineering, 13*(2), 591-599.

Saadatmorad, M., Rezaei-Sedehi, E., & Khatir, S. (2024). Crack detection in historic structures using an improved Prewitt filter: Case study of the Historic Si-o-se-pol Bridge in Iran. *Ho Chi Minh City Open University Journal of Science, Journal of Science - Advances in Computational Structures, 14*(1), 3-9.

Saadatmorad, M., Shahavi, M. H., & Gholipour, A. (2024). Damage detection in laminated composite beams reinforced with nano-particles using covariance of vibration mode shape and wavelet transform. *Journal of Vibration Engineering & Technologies, 12*(3), 2865-2875.

Saadatmorad, M., Talookolaei, R. A. J., Pashaei, M. H., Khatir, S., & Wahab, M. A. (2022). Pearson correlation and discrete wavelet transform for crack identification in steel beams. *Mathematics, 10*(15), Article 2689.

Surace, C., & Ruotolo, R. (1994). Crack detection of a beam using the wavelet transform. In *Proceedings-spie the international society for optical engineering* (vol. 1141). Spie International Society for Optical.

Yu, S. N., Jang, J. H., & Han, C. S. (2007). Auto inspection system using a mobile robot for detecting concrete cracks in a tunnel. *Automation in construction, 16*(3), 255-261.